Materials Science & Engineering A 767 (2019) 138444

Contents lists available at ScienceDirect

Materials Science & Engineering A

journal homepage: http://www.elsevier.com/locate/msea

# Detwinning behavior in commercial pure zirconium during orthogonal re-compression after pre-compression and annealing

Xin Chen [a], Qinghui Zeng [b], Weijun He [a,c,*], Qing Liu [a]

[a] College of Materials Science and Engineering, Chongqing University, Chongqing, 400044, China
[b] College of Intelligent Manufacturing Engineering, Chongqing University of Arts and Sciences, Chongqing 402160, China
[c] International Joint Laboratory for Light Alloys (Ministry of Education), College of Materials Science and Engineering, Chongqing University, Chongqing, 400044, China

ARTICLE INFO

*Keywords:*
Zr alloy
Detwinning
Annealing behavior
Texture

ABSTRACT

Twinning is an important plastic deformation mode for zirconium (Zr) and its alloys. Many researches have been carried out to investigate twinning related issues for Zr alloys. However, few study was reported on the detwinning in Zr alloys. In this work, pre-compression, orthogonal re-compression, and annealing were performed to investigate the deformation behavior of a commercial pure Zr (Zr702). Microstructure and texture evolution during deformation and annealing were examined by quasi-in situ electron backscatter diffraction (EBSD). It was found that {10–12} tensile twins were activated during pre-compression of Zr702 plate along rolling direction, while detwinning rather than secondary tensile twinning occurred when the pre-twinned sample was re-compressed along normal direction. Intermediate annealing between the pre-compression and the re-compression may hinder the subsequent detwinning. Moreover, the hindering effect was enhanced when larger pre-compression and longer annealing time were applied, which may be attributed to the annealing induced solute atoms precipitation and coherency loss of twinning boundary.

## 1. Introduction

Zirconium (Zr) and its alloys are widely applied in nuclear power industry because of their great corrosion resistance, good mechanical properties, and low thermal neutrons absorption cross-section [1,2]. Zr has a hexagonal close-packed (HCP) crystal structure at room temperature. Due to the low symmetry of the HCP crystal structure and the insufficient independent slip systems, plastic deformation of Zr is often accommodated by twinning when the initial orientation is unfavorable for slip [3,4]. Hence, twinning is an important plastic deformation mode for Zr and its alloys. The most commonly reported primary twin modes in Zr are {10–12}<-1011>, {11–21}<-1-126>, {11–22}<-1-123>and {10–11}<-1011> [5,6]. The former two are generally denoted as tensile twins since they are formed when the *c-axis* is elongated. The latter two are called as compressive twins because they are formed when the *c-axis* is contracted [6]. The four twins reorient the crystal lattice by ~85.2° about the {11–20} axis, ~34.8° about the {10-10} axis, ~64.2° about the {10-10} axis, and ~57.1°about the {11–20} axis, respectively [7,8]. Therefore, the activation of twins will change the texture significantly. The evolution of the texture will have great influence on the performance of zirconium alloys, for instance, mechanical properties [9,10], creep [11,12], orientation of hydride [13,14] and corrosion behaviors [15–17].

Many studies have been conducted to investigate the twinning related issues in Zr alloys [7,18–24]. J.H. Chung et al. proposed a method for preparing high volume fraction twins in Zr alloy, and reported that the micro-hardness of the Zr alloy increased with the increase of twins area fraction due to the obstruction effect of twin boundary for dislocations slip [18]. Marko Knezevic et al. studied the strain rate and temperature dependence of twinning and secondary twinning in high-purity Zr, and found that all of studied twin modes were rate insensitive [19]. Statistical investigation by L. Capolungo et al. [7] show that there was a strong correlation between the activated twin variant and the crystallographic orientation. Smaller grain boundary misorientation angles was weakly preferred for the twin activation [7]. J. P. Escobedo et al. found that the extrusion deformation of Zr was accomplished by a combination of twinning and slip [20]. The relative contribution of twinning and slip depended on the initial texture [20]. R. J. McCabe et al. reported that the prismatic slip and the first generation {10–12} tensile twins were the primary deformation mechanisms for the compression along the direction that perpendicular to the *c-axis*, and the contribution of the first generation {11–21} tensile twins was relative

* Corresponding author. College of Materials Science and Engineering, Chongqing University, Chongqing 400044, China.
*E-mail address:* weijun.he@cqu.edu.cn (W. He).

https://doi.org/10.1016/j.msea.2019.138444
Received 31 July 2019; Received in revised form 20 September 2019; Accepted 21 September 2019
Available online 22 September 2019
0921-5093/

smaller [21]. The previously stored dislocation did not significantly change the growth of the {10–12} twins, but it promoted the resistance to the propagation of {11–22} twins [22]. More coherency losses of the twin boundary and a higher diving force in the sample with a larger pre-annealing deformation can enhance twin boundary migration at lower annealing temperatures [23,24]. Above all, most of researches focused on twinning in Zr alloy. However, few investigation on detwinning of Zr alloy has been reported.

Under suitable load conditions, the twin generated previously can be receded. This process was generally named as detwinning. Detwinning can be roughly treated as twinning again on a pre-twin, which leading to an orientation just as the matrix [25,26]. Detwinning was a process controlled by the migration of the twin boundary [25,27]. Magnesium (Mg) alloys have HCP structure as Zr alloys. For Mg alloys, detwinning as well as twinning are also important plastic deformation modes. As an example, detwinning were often observed during in-plane tension after in-plane pre-compression in an Mg sheet with strong basal texture [27]. The activation of {10–12} twinning and detwinning would greatly contribute to the evolution of the texture and microstructure of Mg alloy [27,28], thus having a significant effect on the mechanical properties. In addition, Nie et al. [29] demonstrated that the quick segregation of solute atoms at fully coherent terraces of twin boundaries (TBs) occurred during annealing of Mg alloy. And, the segregated solute at TBs will pin TB migration, which cause an annealing hardening in Mg alloy [28]. It is not clear whether annealing will affect the detwinning of Zr alloy or not. Nevertheless, much work need to been done to investigate the detwinning related issues in Zr alloy.

In this work, pre-compression along rolling direction (RD) was used to activate twinning in a Zr alloy plate, which was followed by re-compression along normal direction (ND). Detwinning was observed during the re-compression along ND. In addition, intermediate annealing was also performed for some samples. The motivation of this study is to study the detwinning behavior in Zr alloy and the effect of annealing on the detwinning.

## 2. Experiments

A commercial pure Zr (Zr702) plate, with initial thickness of 4 mm, was used as the experimental material in this study. The as-received plate has a full recrystallization microstructure, and the initial average grain size is approximately 25 μm, which was measured by linear intercept method, as shown in Fig. 1. It can be found that the initial microstructure is free from twin, as indicated in the boundary map and the misorientation distribution map (Fig. 1(b) and (d)). In the boundary map, high angle grain boundary (misorientation angle >10°) and low angle grain boundary (2° < misorientation angle <10°) are represented by dark coarse line and gray fine line, respectively. {10–12} tensile twin boundary is marked with red solid line. The initial texture is a kind of basal texture, which is a kind of typical texture in rolled Zr alloy sheet.

Small samples, with size of 6 (along RD) × 5 mm (along transvers direction, TD). were cut from the as-received Zr702 plate to carry out the pre-compression and re-compression. Compression process is schematically shown in Fig. 2. The pre-compression was along RD to active {10–12} tensile twins, then the pre-twinned sample were re-compressed along ND to investigate the detwinning. Two levels of strains, 5% and 10%, were applied in the pre- and re-compression. The compressions

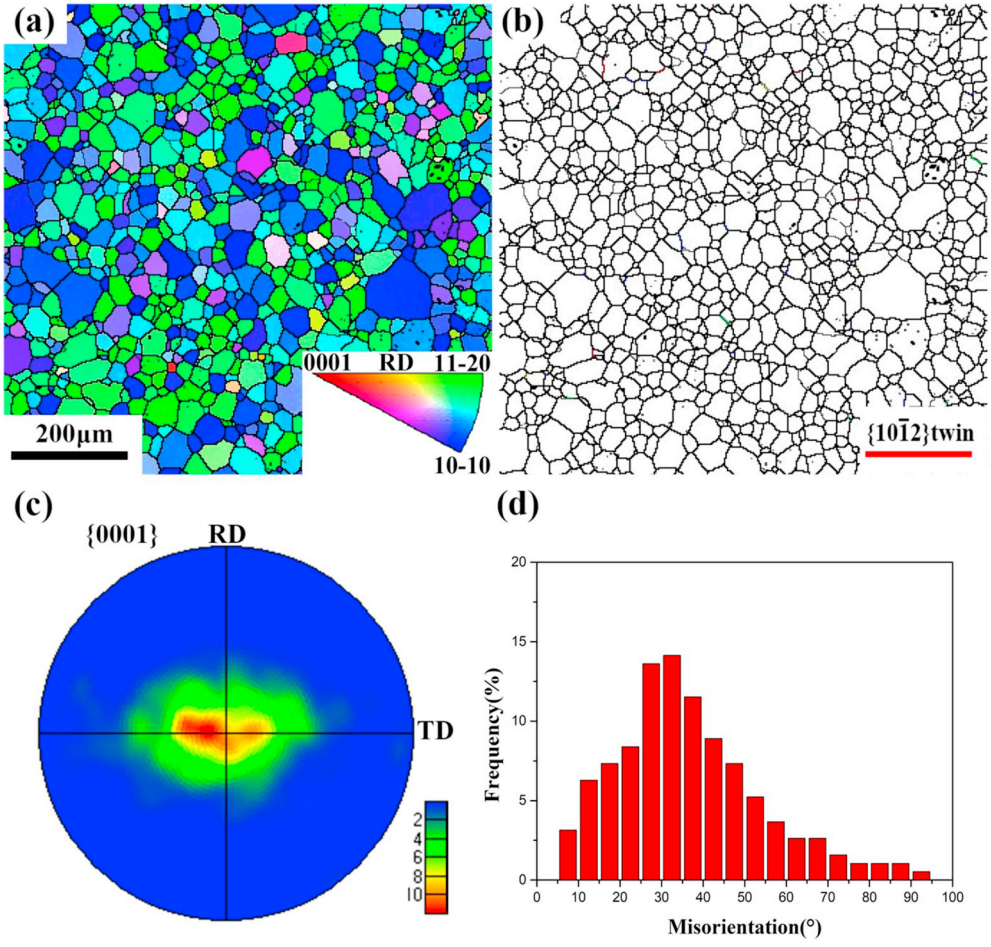


**Fig. 1.** Initial microstructure of the experimental material: (a) orientation imaging map (b) boundaries map, (c) {0001} pole figure and (d) misorientation angle distribution.

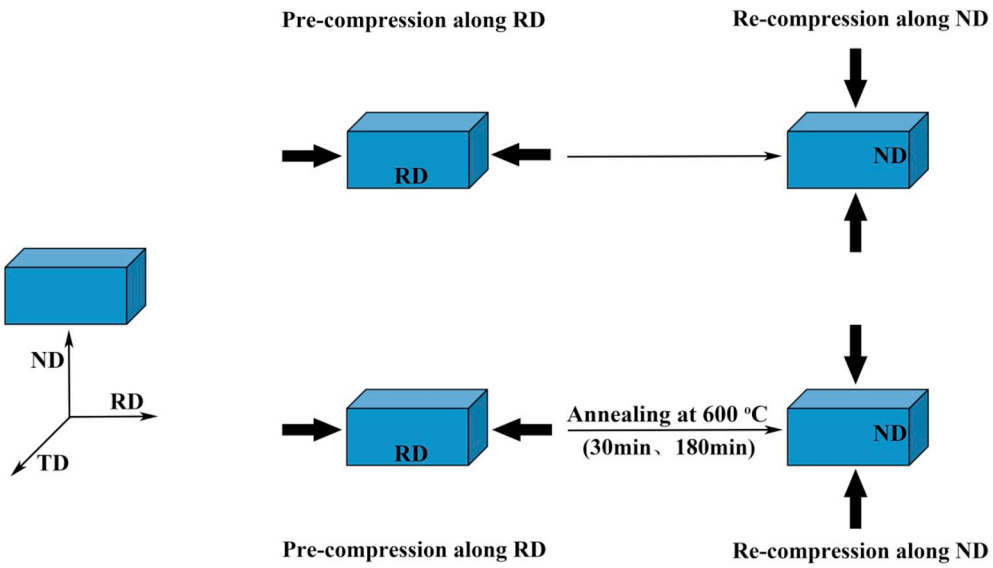


**Fig. 2.** Schematically illustration of pre-compression, annealing and re-compression.

were conducted on an AGX-50kN machine at room temperature with a strain rate of $\sim 10^{-2}$ $s^{-1}$. Between the pre-compression and the re-compression, annealing was performed for some samples. Annealing was performed at 600 °C for 30 minutes or 180 minutes. Annealing was carried out in a vacuum furnace. For convenience, the samples at different states were named after the deformation and annealing history. For example, the CR-10%-A180-CN-10% represents the sample that was pre-compressed 10% along RD and subsequently annealed at 600 °C for 180 minutes, and then re-compressed 10% along ND.

Representative engineering stress-strain curves of the compression are shown in Fig. 3. It can be seen that the flow stress along ND compression is obvious higher than that along RD, which is mainly caused by the texture induced anisotropy. However, the flow stress of CR-10%-A30-CN-10% and CR-10%-A180-CN-10% are higher than that of CR-10%–CN–10%. This phenomenon is not consistent with the traditional annealing induced softening effect, which implies different deformation mechanisms occurred between the annealed and un-annealed samples.

The microstructure and texture evolution during deformation and annealing were characterized by electron backscatter diffraction (EBSD), using an TescanMir3 Field emission scanning electron microscope equipped with an Oxford Instruments-HKL Technology Nordlys EBSD system. The indexing step size used to capture EBSD images was 1.5 μm, and the examined area was 400 × 400 μm. Pole figures and

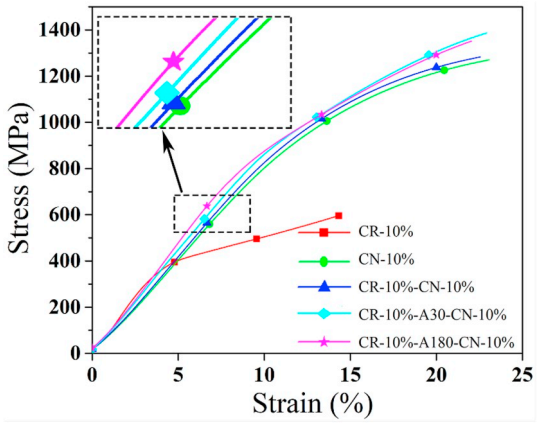


**Fig. 3.** Engineering stress-strain curves of pre-compression and re-compression.

boundary information were analyzed by commercial available package Channel 5.

## 3. Results

### 3.1. Microstructure of the pre-compressed samples

Orientation imaging maps and boundary maps of Zr702 after 5% and 10% pre-compression along RD are shown in Fig. 4. It indicates that some twins are observed after 5% pre-compression along RD, as shown in Fig. 4(a). These twins are identified as {10–12} tensile twins based on the special rotation axis-angle information of the twin boundary, as marked with red boundaries in Fig. 4(c). For the applied uniaxial compressive deformation along RD, it tends to cause tensile deformation along ND. In addition, most of the *c-axis* are aligned along ND according to the initial basal texture of the used Zr702 plate. So, it is reasonable to activate the {10–12} tensile twin during RD compression. Indeed, the activation of {10–12} tensile twinning during the RD compression of a rolled Zr-4 alloy sheet has also been reported in our previous studies [23, 24].

With the increase of the applied strain, more twin lamellar are noted, as indicated in Fig. 4(b) and (d). Moreover, twin lamellar in CR-10% sample get thicker compared with that in CR-5%. Color (orientation) gradient, which is generally related with the accumulation of dislocation slipping [22], can be noted in some grains, as shown in Fig. 4(b). That implies there are also dislocations slipping to accommodate to the compression deformation along RD in addition to the activation of the {10–12} tensile twins. The shear strain of the {10–12} tensile twinning is 0.167 [30], and the area fraction of the activated {10–12} twins is ~7% in the CR-10% sample. So, the maximum strain accommodated by the tensile twinning is ~1.16%, which is much less than the applied 10% strain. Most of the applied strain is accommodated by dislocation slipping.

### 3.2. Detwinning during re-compression

Orientation imaging maps and boundary maps of CR-5%–CN–5% sample and CR-10%–CN–10% sample, which are re-compressed along ND on the base of the pre-twinned sample, are presented in Fig. 5. After re-compression along ND, Fig. 5 indicates that no twin lamellar and no {10–12} tensile twin boundary can be observed despite the applied strain. It is expected that detwinning has happened during the re-compression along ND.

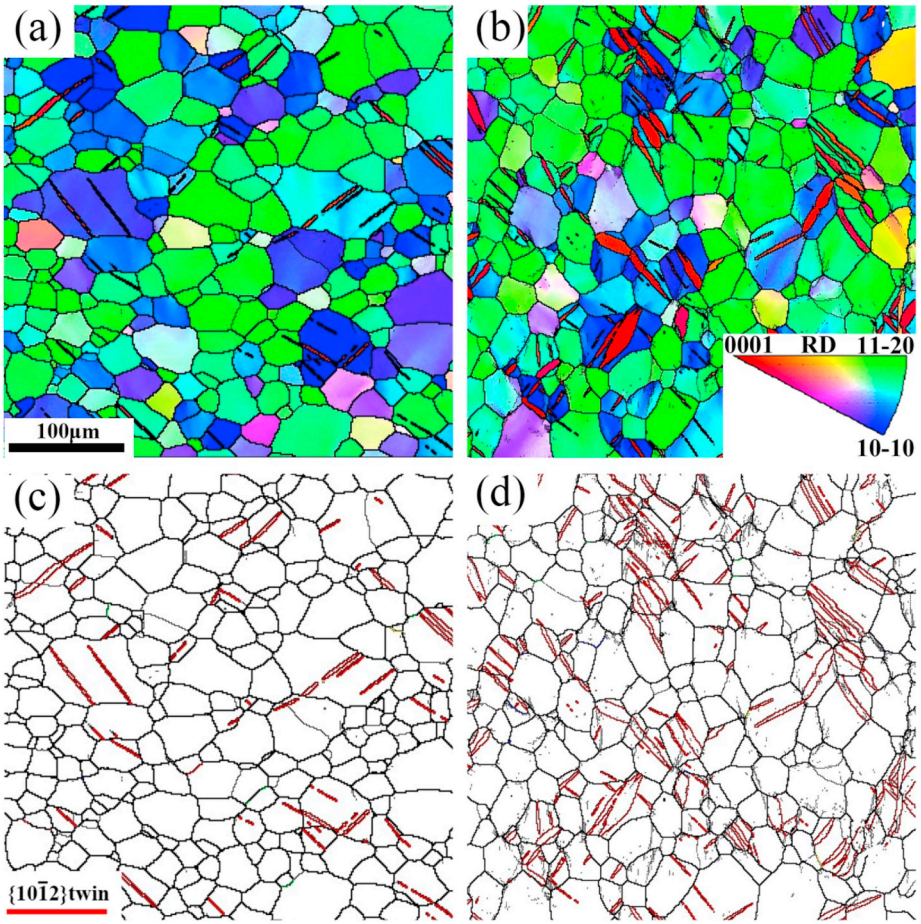


**Fig. 4.** Microstructures of pre-compressed samples: orientation imaging maps of (a) CR-5% and (b) CR-10%, and boundary distributions of (c) CR-5% and (d) CR-10%.

To further confirm whether the detwinning happened or not, quasi-in-situ EBSD observations were carried out. Before any compression, the RD-ND surface of a Zr702 sample was prepared for EBSD observations. Then, four indentations were carefully introduced by micro-hardness tests to make sure that the same local region can be found in different EBSD observations. Before the pre-compression along RD, the first time of EBSD observation was carried out. Then, after the pre-compression (un-loading), the second time of EBSD observation was performed in the same region as that in the first time of EBSD observation. The third time of EBSD observation in the same region was conducted after the re-compression along ND (un-loading). It is worthy to note that no additional polishing procedure was added between different EBSD observations.

Fig. 6 displays the EBSD maps before and after the pre- and re-compression. As mentioned also in 3.1 section, {10–12} tensile twinning is activated during the pre-compression along RD, as indicated in Fig. 6(a) and (b). For some grains, no twinning is activated, which may be attributed to the unfavorable initial orientation and local stress state. After the re-compression along ND, all twin lamellar and twin boundaries are disappeared, as shown in Fig. 6(c) and (f). The orientation of the pre-twinned area return to the orientation of matrix, as shown in Fig. 7. Therefore, it is reasonable to expect that detwinning has occurred during the re-compression along ND.

Detwinning were often reported to activate during the loading and reverse loading of HCP metals, for example Mg alloy and Zr alloy [26,27,31,32]. However, detwinning is observed during orthogonal re-compression after pre-compression along RD, which is not reported before. The activation of detwinning in current loading path may be related with its low critical resolved shear stress, which will be further discussed in section 4.1.

### 3.3. *Effect of intermediate annealing on the detwinning*

Microstructures of Zr702 after pre-compression along RD and annealing at 600 °C for 180 minutes are shown in Fig. 8. It is worth to note that the often used recrystallization annealing process of Zr702 is held at 600 °C for 60 minutes [33]. Fig. 8 reveals that the activated twins are reserved after the recrystallization annealing treatment despite of the pre-strain. Twin boundary is a kind of coherent boundary [23,34,35], which is very stable during annealing treatment. Our previous studies indicated that large pre-annealing deformation and high temperature were needed to cause thermally activated twin boundary migration for Zr-4 alloy [23,24]. No obvious thermally activated twin boundary migration is noted in current annealing, which may be attributed to the applied small pre-annealing deformation (≤10%).

Orientation imaging maps and boundary maps of Zr702 samples with intermediate annealing between the re-compression along ND and pre-compression along RD are presented in Fig. 9 and Fig. 10. For CR-5%-A30-CN-5%, no twin lamellar can be observed. Compared with CR-5%-A180 sample (Fig. 8), in which the twin lamellar are retained after annealing for 180 minutes, it is reasonable to speculate that the disappear of twin lamellar in CR-5%-A30-CN-5% is caused by detwinning during the re-compression. The microstructure of CR-5%-A30-CN-5% is similar with that in CR-5%–CN–5%, which implies that the intermediate annealing for 30 minutes has no significant effect on the detwinning. However, when the intermediate annealing time is 180 minutes, some twin lamellar are remained in CR-5%-A180-CN-5%, as shown in Figs. 9 (b) and Fig. 10(b). That means long time annealing may hinder the

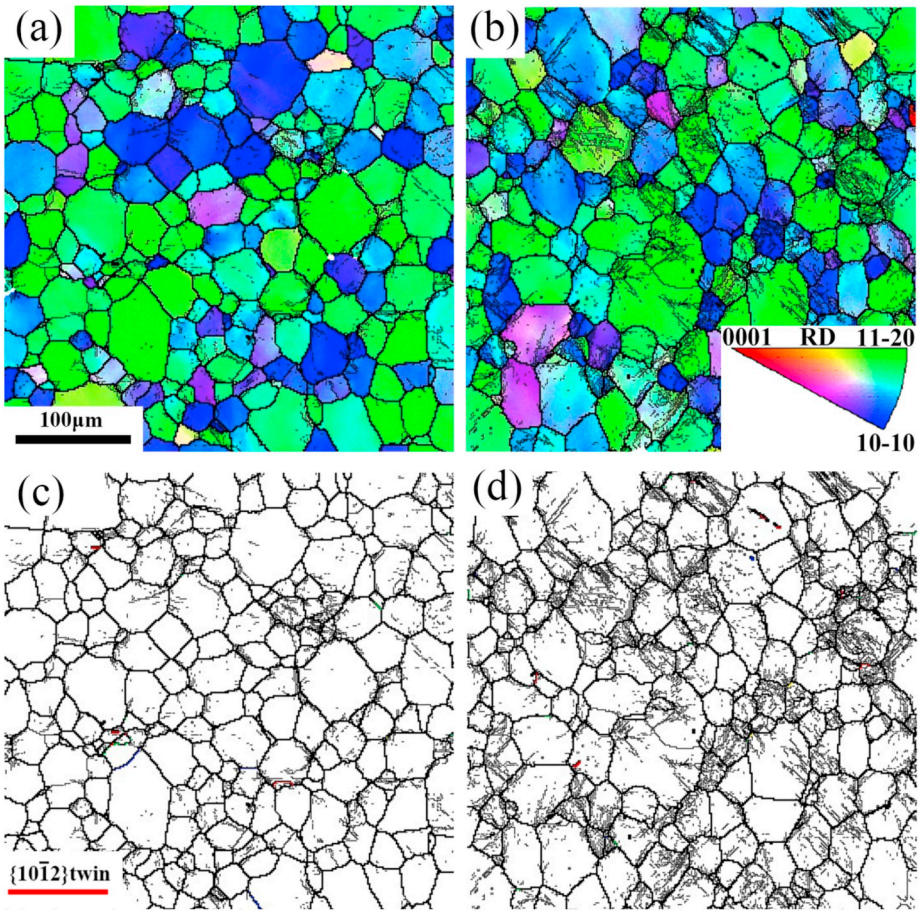


**Fig. 5.** Microstructures of re-compressed samples without intermediate annealing: orientation imaging maps of (a) CR-5%–CN–5% and (b) CR-10%–CN–10%, and boundary distributions of (c) CR-5%–CN–5% and (d) CR-10%–CN–10%.

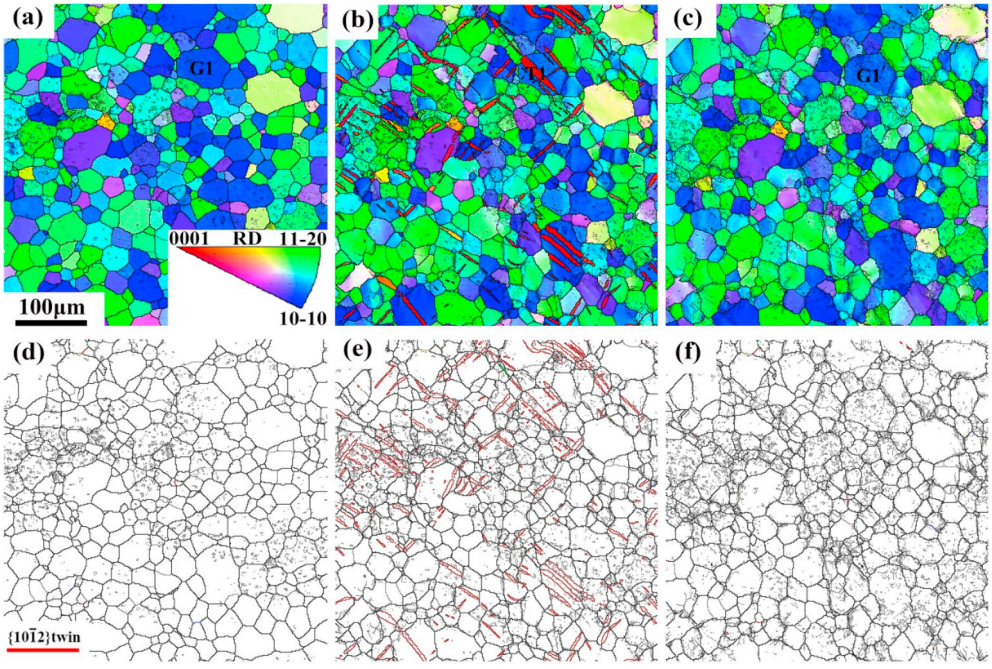


**Fig. 6.** Microstructure by Quasi-in situ observation at different states: orientation imaging maps (a) as-received, (b) CR-10% and (c) CR-10%–CN–10%, and boundary distributions of (a) as-received, (b) CR-10% and (c) CR-10%–CN–10%.

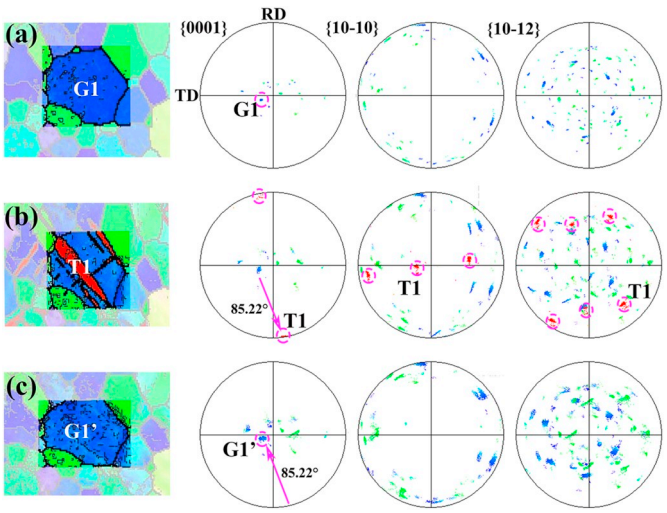


**Fig. 7.** Quasi-in-situ orientation analysis of typical matrix and twins (a) as-received, (b) CR-10% and (c) CR-10%–CN–10%.

detwinning.

When the applied strain is 10%, annealing at 600 °C for 30 minutes show hindering effect for the detwinning since many twin lamellar can be found in CR-10%-A30-CN-10% sample, as shown in Figs. 9(c) and Fig. 10(c). With the increase of annealing time, Figs. 9(d) and Fig. 10(d) show that more twin lamellar are remained. In summary, intermediate annealing may hinder the detwinning behavior during orthogonal re-compression of Zr702. And, the hindering effect becomes more prominent with the increase of the applied strain and the annealing time. The hindrance effect of annealing to detwinning may be related to solute atoms precipitation and recovery, which have been mentioned in Mg alloys [28], and will be further discussed in section 4.2.

### 3.4. Evolution of twin area fraction and texture

To further illustrate the evolution of twins, the twin's number and area fractions in different samples are counted, as shown in Fig. 11. It can be seen that the area fraction of twin increases with the rise of pre-compression. The twin area fraction reaches ~7% for CR-10%. The annealing at 600 °C will not reduce or increase the area fraction of the pre-twins despite of the applied deformation. Without intermediate annealing, equal re-compressive deformation (as that in pre-compression along RD) along ND will cause a full detwinning, thus leading to the disappearance of twin. When the applied strain is 5%, annealing for 30 minutes can not hinder the detwinning in re-compression. While, annealing for 180 minutes can retain ~75% of the twins. When the applied strain is 10%, annealing for 30 minutes and 180 minutes have remained ~20% and ~50% of the pre-twins, respectively.

To investigate the texture evolution, {0001} pole figure of samples were measured by EBSD, as shown in Fig. 12. For samples with 5% deformation, the influence of twinning, annealing and detwinning on the orientation of *c-axis* is weak due to small area fraction of twin. For samples with 10% pre-compression along RD, a new texture component {0001}||RD arises, which is caused by the activation of {10–12} tensile twinning [23,24]. The occurrence of {10–12} tensile twins causes the

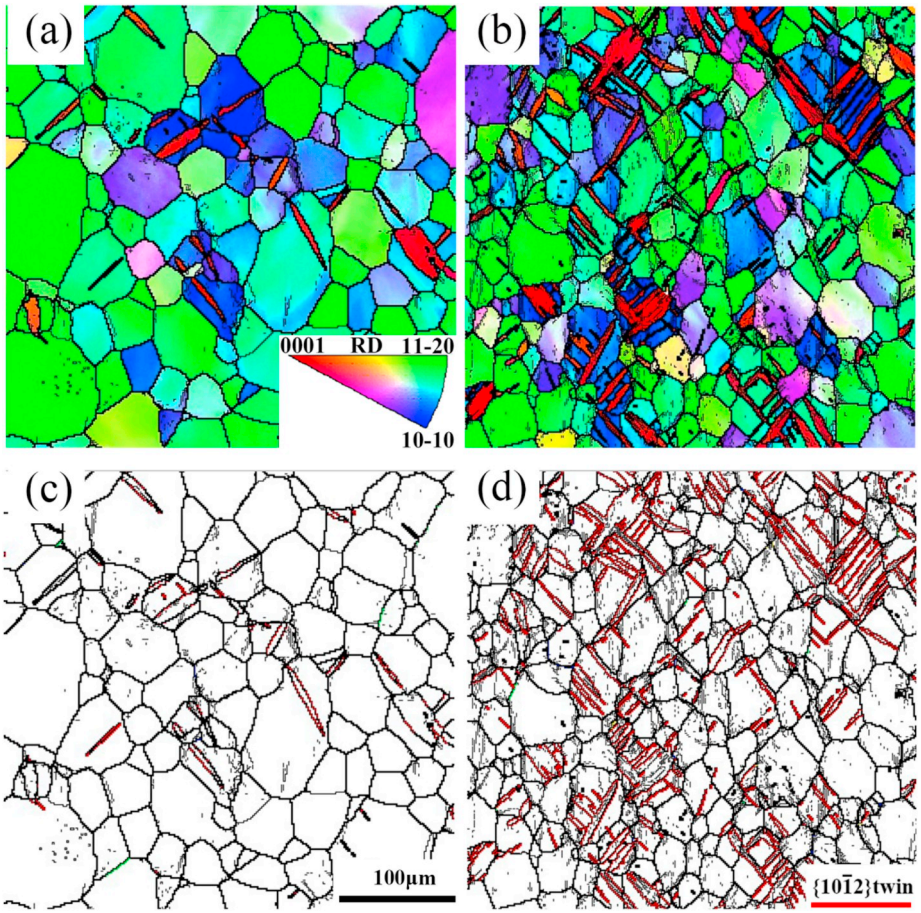


**Fig. 8.** Microstructures of pre-compressed and annealed samples: orientation imaging maps (a) CR-5%-A180 and (b) CR-10%-A180, and twin boundary distribution of (c) CR-5%-A180 (d) CR-10%-A180.

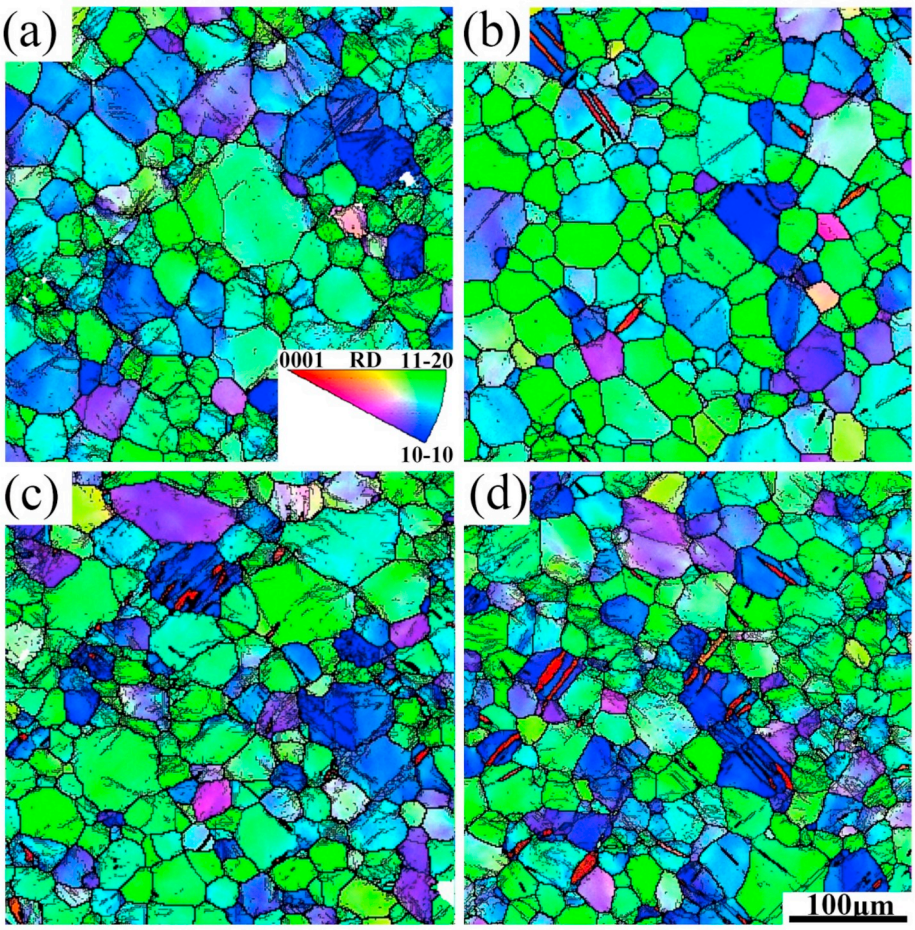


**Fig. 9.** Orientation imaging maps of re-compressed sample with intermediate annealing: (a) CR-5%-A30-CN-5%, (b) CR-5%-A180-CN-5%, (c) CR-10%-A30-CN-10% and (d) CR-10%-A180-CN-10%.

*c-axis* of rotate by ~85.2° [5,8,23]. After annealing, the twin induced texture component {0001}||RD is kept, as show in the CR-10%-A180 sample. While, in the {0001} pole figure of the sample CR-10%–CN–10%, the twin induced texture component {0001}||RD is disappeared, which is caused by the detwinning and is consistent with the mentioned microstructure evolution (Fig. 5). With intermediate annealing between the pre-compression along RD and re-compression along ND, the twin induced texture component {0001}||RD can be still noted although the intensity is weaken, as indicated in the CR-10%-A180-CN-10% sample.

## 4. Discussion

### 4.1. Detwinning rather than secondary twinning in re-compression

Based on the initial {0001} pole figure of the used material (Fig. 1 (c)), the initial orientation of the *c-axis* is mainly orientated along the ND. After pre-compression along RD, the activation of {10–12} tensile twins rotate the *c-axis* to align with RD, as mentioned in section 3.2 and show in Fig. 7. Then, during the re-compression along ND, there is a tendency to cause tensile deformation along RD, which may activate secondary {10–12} twinning as well as detwinning for the pre-twinned grain, as schematically shown in Fig. 13. However, the experimental results indicate that only detwinning was activated during the re-compression along ND.

It was reported that detwinning was achieved by the migration of twin boundary [25,27]. While, the activation of twinning needs two process, nucleation and propagation. Relative high stress was needed for the nucleation of a new twin. So, detwinning is to occur at lower applied stress than twinning [26,36]. Therefore, under same other condition, detwinning is preferred than twinning, which may be one of the most important reason for the detwinning activation in the re-compression of Zr702. In addition, the re-compression along ND tends to activate secondary twinning in the primary twins. However, the thickness of the primary twins is smaller than the grain size of matrix, as shown in Fig. 4. It was reported that twinning is size sensitive and larger grain size was favorable for the twinning, which was confirmed in our previous study [23]. So, the small thickness of the primary twins may further constrain the activation of the potential secondary twining during the re-compression along ND.

### 4.2. Effect of annealing on the subsequent detwinning

Fig. 9 indicates that annealing may hinder the subsequent detwinning in Zr702. This is also validated by the lower flow stress for samples with intermediate annealing, as shown in Fig. 3. Generally, annealing causes softening effect for a cold deformed metallic sample. However, Fig. 3 indicates that samples with intermediate annealing show higher flow stress than that sample without annealing. This can be explained by the annealing induced hindering effect for detwinning. Since detwinning (with relative lower activation stress) is hindered, other deformation mechanisms (with relative higher activation stress) are needed, thus leading to the higher flow stress. In addition, as indicated in Fig. 9, the hindering effect of annealing is enhanced with larger pre-compression deformation and longer annealing time. Annealing may cause segregation of solute atoms at the twin boundaries and destruct the coherency of

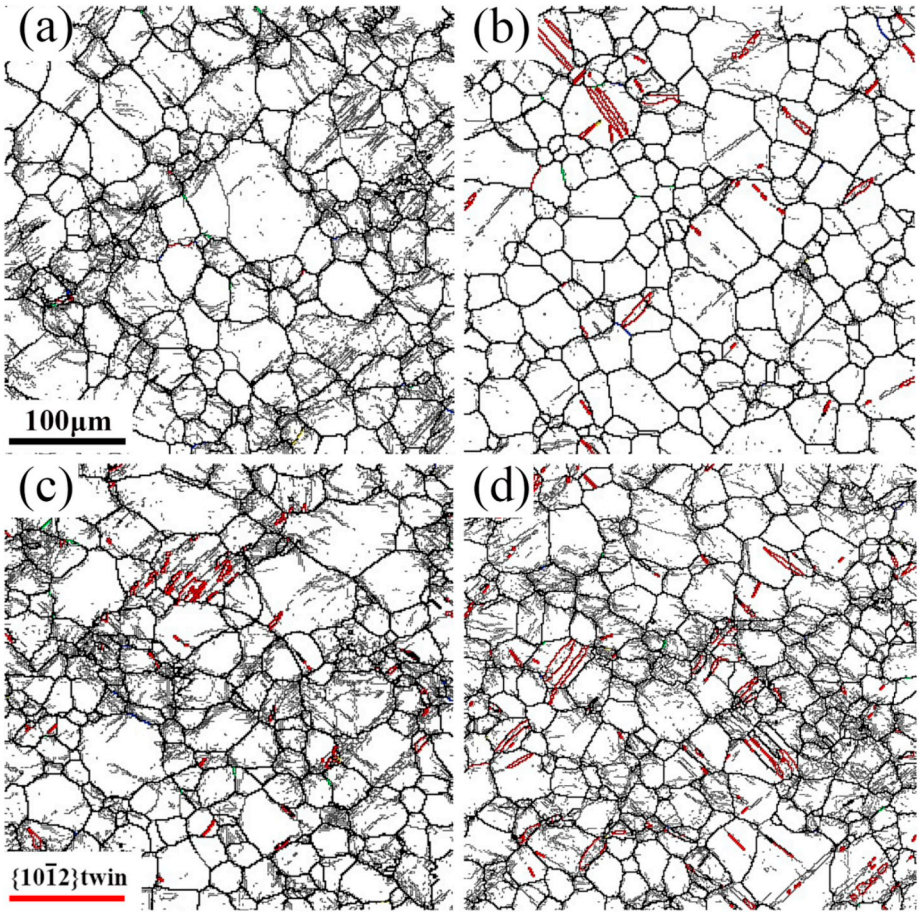


**Fig. 10.** Boundary distributions maps of re-compressed samples with intermediate annealing: (a) CR-5%-A30-CN-5%, (b) CR-5%-A180-CN-5%, (c) CR-10%-A30-CN-10% and (d) CR-10%-A180-CN-10%.

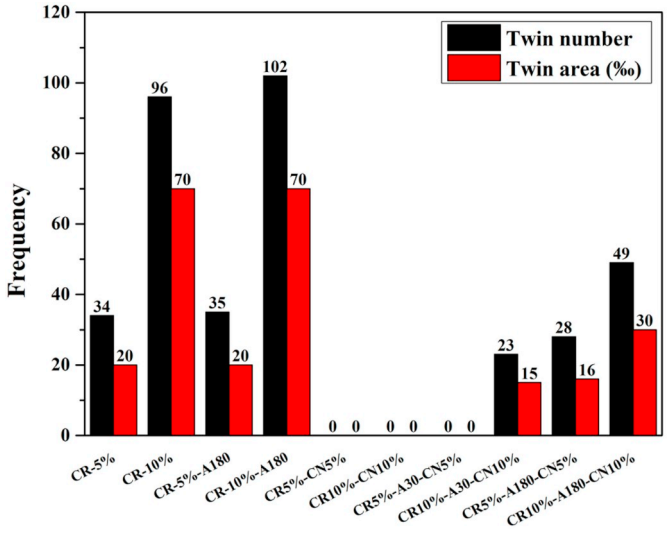


**Fig. 11.** Quantitative statistics of the number and area fraction of the tensile twins.

the twin boundary, thus influencing the detwinning.

The used material in current study is commercial pure Zr702. Impurity atoms, for example Hf, Fe and Cr, are contained in the used material. During annealing at 600 °C, which is higher than the recrystallization temperature, the solid solution atoms may segregate at the twin boundaries. For Mg alloy, Nie et al. [29] found the segregation of solute atoms at twin boundaries during annealing process. The segregated solute at twin boundaries will pin twin boundaries migration and improve the stability of twins, which lead to the detwinning more difficult to take place. Xin et al. [28] also revealed that the solute atoms can pin twin boundaries migration and impede the detwinning. So, it is expected that the segregation of Hf, Fe and Cr atoms at the {10–12} twin boundaries increase the stability of twin boundary, which is not favorite for the detwinning. Since the segregation of solid atoms is a diffusion-dominated process, a certain time is needed to accomplish the segregation, which explains why the hindering effect of annealing is enhanced with longer annealing time.

Moreover, the coherency of the twin boundary may be partly destructed during annealing, which is also not beneficial for the subsequent detwinning. Fig. 14(a) is a typical twin-matrix pair in CR-10% sample. Misorientaion angles around the twin boundary are measured and marked. In different local regions, the misorientation angles are inconsistent. The minimum misorientation angle is 83.9°, and the largest misorientation angle is 89.9°. Theoretically, the misorientation angle of {10–12} twin boundaries should be ~85.2°. Fig. 14(a) indicates that the misorientation angle of the twin boundary after annealing deviates from the theoretical value even considering the accuracy of the EBSD detection (maximum deviation of 2°), which demonstrates the destruction of coherency.

To further illustrate the loss of coherency of twin boundaries during annealing, the distribution of twin boundary line ratios with different maximum-deviation-angles are counted and displayed in Fig. 14(b). The twin boundary line ratio is defined as the ratio of twin boundary to the high angle (≥10°) boundary. When smaller maximum-deviation-angle is used, the rotation axis-angle pair of the indexed twin boundaries is more

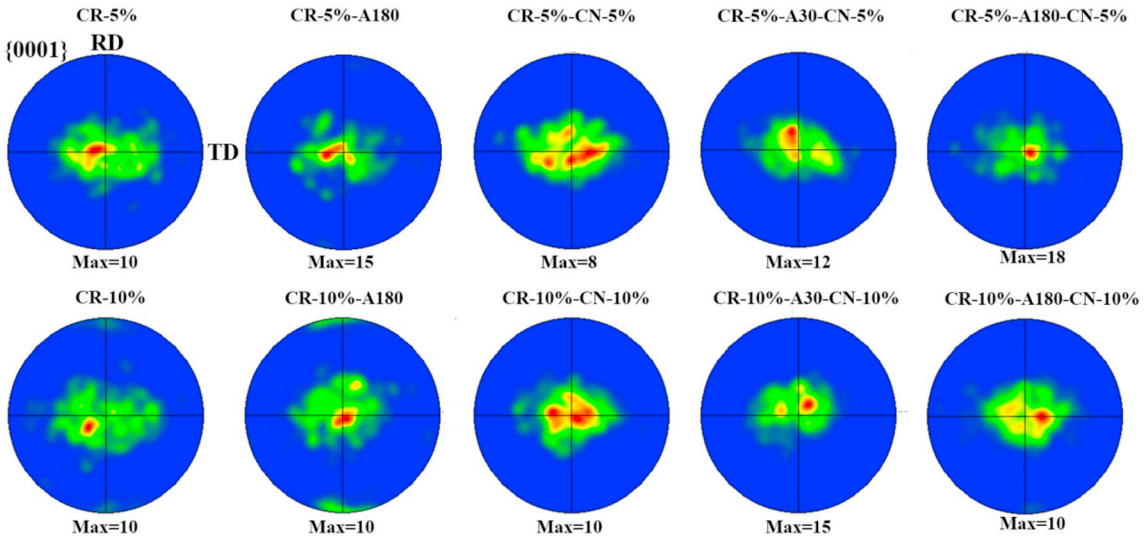


**Fig. 12.** Texture evolution during deformation and annealing.

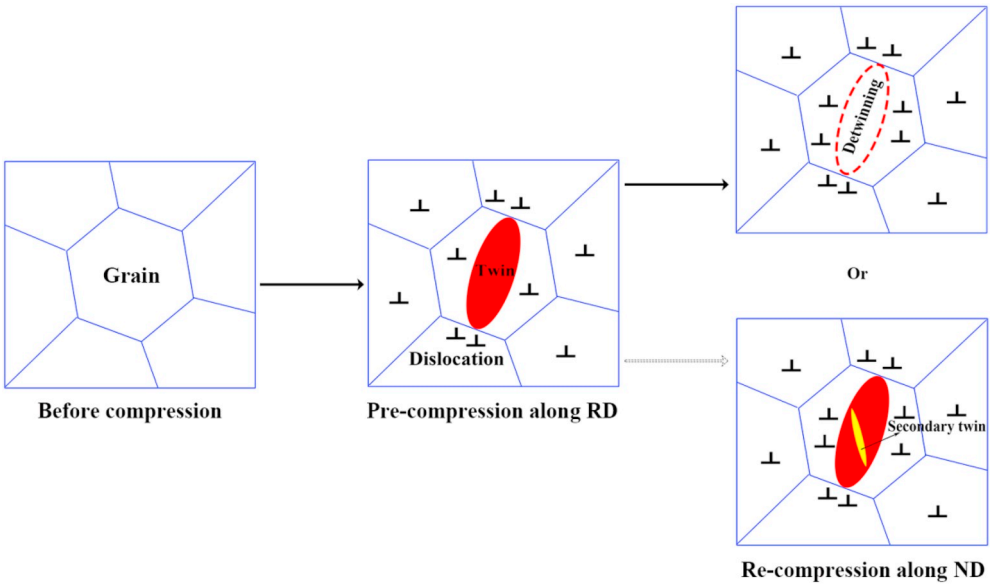


**Fig. 13.** Schematically illustration on possible deformation modes (detwinning or secondary twinning) during re-compression along ND after pre-compression along RD.

close to the theoretical value. Theoretical twin boundary is a kind of coherent boundary. So, when changing from high maximum-deviation-angle to low value, the smaller the decrease amplitude of the twin boundary line ratio, the higher the coherency of the twin boundary is. When the maximum-deviation-angle decrease from 5° to 1°, Fig. 14(b) indicates that the twin boundary line ratio decrease from 14.2% to 9.5% and from 13.3% to 1.1% for CR-5% and CR-5%-A180, respectively. That means more coherency is lost after annealing. Comparing CR-10% and CR-10%-A180, same conclusion can be drawn. If the coherency is lost, the twin boundary will transform to an ordinary high angle boundary, which may be not beneficial for the detwinning.

## 5. Conclusions

In this work, re-compression along ND after pre-compression along RD and annealing was carried out to reveal the plastic deformation mechanism of Zr702 plate in complex strain path. Microstructure and texture evolution during deformation and annealing were examined by EBSD. The primary conclusions can be drawn as follows:

(1) {10–12} tensile twins are activated during pre-compression along RD, while detwinning rather than secondary tensile twinning occurs when the pre-twinned sample is re-compressed along ND.
(2) Annealing at 600 °C for 180 min will not cause significant thermally activated twin boundary migration for Zr702 plate with pre-annealing deformation 10%.
(3) Intermediate annealing between the pre-compression and the re-compression may hinder the subsequent detwinning. And, the hindering effect is enhanced when larger pre-compression and longer annealing time are applied. The hindering effect of intermediate annealing on the detwinning may be related with the loss of coherency of twin boundary and the segregation of solid solution atoms at twin boundary during annealing.

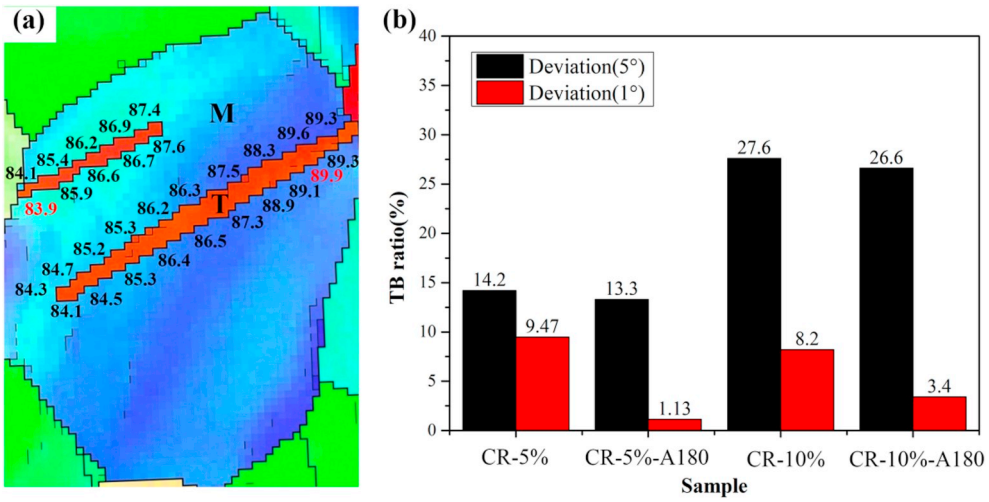


**Fig. 14.** (a) Misorientation angle distribution of twin-matrix pair in a sample of C-RD-10% and (b) twin boundary line ratios with various deviations.

## Data availability

The raw data required to reproduce these findings are available from the corresponding author on reasonable request.

## Acknowledgements

The authors express their sincere thanks for the financial support from the National Natural Science Foundation of China (Projects 51971041, 51601023 and 51421001).

## References

[1] M.K.B.S. Banerjee, Nuclear applications zirconium alloy, Mater. Sci. Mater. Eng. (2016) 6287–6299.
[2] J.A.L. Robertson, Zirconium-an international nuclear material, J. Nucl. Mater. 100 (1981) 108–118.
[3] R.A.L.C.N. Tome, A model for texture development dominated by deformation twinning_ application to zirconium alloys, Acta Metall. Mater. 39 (1991) 2667–2680.
[4] L. Chai, B. Luan, K.L. Murty, Q. Liu, Effect of predeformation on microstructural evolution of a Zr alloy during 550–700°C aging after β quenching, Acta Mater. 61 (2013) 3099–3109.
[5] M. Zhang, B.F. Luan, Z.L. Song, R.L. Xin, K.L. Murty, Q. Liu, {11-21}-{10-12} double twinning in a Zircaloy-4 alloy during rolling at ambient temperature, Scr. Mater. 122 (2016) 77–81.
[6] S.K. Sahoo, V.D. Hiwarkar, K.V. Mani Krishna, I. Samajdar, P. Pant, P.K. Pujari, G. K. Dey, D. Srivastav, R. Tiwari, S. Banerjee, Grain fragmentation and twinning in deformed Zircaloy 2: response to positron lifetime measurements, Mater. Sci. Eng. A 527 (2010) 1427–1435.
[7] L. Capolungo, P.E. Marshall, R.J. McCabe, I.J. Beyerlein, C.N. Tomé, Nucleation and growth of twins in Zr: a statistical study, Acta Mater. 57 (2009) 6047–6056.
[8] B.F. Luan, L.J. Chai, G.L. Wu, H.B. Yu, J.W. Chen, Q. Liu, Twinning during β→α slow cooling in a zirconium alloy, Scr. Mater. 67 (2012) 716–719.
[9] M. Isaenkova, P. Yu, O. Krymskaya, S. Pakhomov, Iop Conference Series Materials Science & Engineering, 2015, 012092.
[10] Z.N. Yang, X.B. Wang, F. Liu, F.C. Zhang, L.J. Chai, R.S. Qiu, L.Y. Chen, Effect of intercritical annealing temperature on microstructure and mechanical properties of duplex Zr-2.5Nb alloy, J. Alloy. Comp. 776 (2019) 242–249.
[11] W.J. Li, R.A. Holt, Effect of texture on anisotropic creep of pressurized Zr-2.5Nb tubes, Mater. Sci. Forum 539 (2009) 3353–3358.
[12] W. Li, R.A. Holt, M.R. Daymond, F. Xu, Influence of prior dislocation structure on anisotropy of thermal creep of cold-worked Zr–2.5Nb tubes, J. Nucl. Mater. 412 (2011) 138–144.
[13] A.T. Motta, L. Capolungo, L.-Q. Chen, M.N. Cinbiz, M.R. Daymond, D.A. Koss, E. Lacroix, G. Pastore, P.-C.A. Simon, M.R. Tonks, B.D. Wirth, M.A. Zikry, Hydrogen in zirconium alloys: a review, J. Nucl. Mater. 518 (2019) 440–460.
[14] S.-D. Kim, J.-S. Kim, J. Yoon, Phase analysis of hydride blister in zirconium alloy, J. Alloy. Comp. 735 (2018) 2007–2011.
[15] S. Xie, B. Zhou, X. Liang, W. Liu, H. Li, Q. Li, M. Yao, J. Zhang, A novel mechanism for nodular corrosion of Zircaloy-4 corroded in 773 K superheated steam, Corros. Sci. 126 (2017) 44–54.
[16] M.K.B.S. Banerjee, Corrosion of zirconium and its alloys, Mater. Sci. Mater. Eng. (2016) 6287–6299.
[17] M.Y. Yao, Y.F. Shen, Q. Li, J.C. Peng, B.X. Zhou, J.L. Zhang, The effect of final annealing after β-quenching on the corrosion resistance of Zircaloy-4 in lithiated water with 0.04M LiOH, J. Nucl. Mater. 435 (2013) 63–70.
[18] J.H. Chung, Development of thermomechanical processing method to enhance twinning in commercially pure Zr, Scr. Mater. 61 (2009) 161–164.
[19] M. Knezevic, M. Zecevic, I.J. Beyerlein, J.F. Bingert, R.J. McCabe, Strain rate and temperature effects on the selection of primary and secondary slip and twinning systems in HCP Zr, Acta Mater. 88 (2015) 55–73.
[20] J.P. Escobedo, E.K. Cerreta, C.P. Trujillo, D.T. Martinez, R.A. Lebensohn, V. A. Webster, G.T. Gray, Influence of texture and test velocity on the dynamic, high-strain, tensile behavior of zirconium, Acta Mater. 60 (2012) 4379–4392.
[21] R.J. McCabe, G. Proust, E.K. Cerreta, A. Misra, Quantitative analysis of deformation twinning in zirconium, Int. J. Plast. 25 (2009) 454–472.
[22] L. Capolungo, I.J. Beyerlein, G.C. Kaschner, C.N. Tomé, On the interaction between slip dislocations and twins in HCP Zr, Mater. Sci. Eng. A 513–514 (2009) 42–51.
[23] W. He, X. Chen, H. Chen, Q. Liu, Grain size effect on the thermally activated twin boundary migration in a zirconium alloy, Mater. Sci. Eng. A 724 (2018) 576–585.
[24] W. He, X. Chen, Q. Liu, Effect of pre-annealing deformation on thermally activated twin boundary migration in a zirconium alloy, J. Alloy. Comp. 742 (2018) 29–37.
[25] C.J. Geng, B.L. Wu, X.H. Du, Y.D. Wang, Y.D. Zhang, F. Wagner, C. Esling, Low cycle fatigue behavior of the textured AZ31B magnesium alloy under the asymmetrical loading, Mater. Sci. Eng. A 560 (2013) 618–626.
[26] G. Proust, G.C. Kaschner, I.J. Beyerlein, B. Clausen, D.W. Brown, R.J. Mccabe, C. N. Tomé, Detwinning of high-purity zirconium: in-situ neutron diffraction experiments, Exp. Mech. 50 (2010) 125–133.
[27] H. Yu, Y. Xin, H. Zhou, R. Hong, L. Zhao, Q. Liu, Detwinning behavior of Mg–3Al–1Zn alloy at elevated temperatures, Mater. Sci. Eng. A 617 (2014) 24–30.
[28] Y. Xin, X. Zhou, H. Chen, J.-F. Nie, H. Zhang, Y. Zhang, Q. Liu, Annealing hardening in detwinning deformation of Mg–3Al–1Zn alloy, Mater. Sci. Eng. A 594 (2014) 287–291.
[29] J.F. Nie, Y.M. Zhu, J.Z. Liu, X.Y. Fang, Periodic segregation of solute atoms in fully coherent twin boundaries, Science 340 (2013) 957–960.
[30] E. Tenckhoff, Deformation Mechanisms, Texture, and Anisotropy in Zirconium and zircaloy[J], 1980.
[31] Y. Xin, X. Zhou, L. Lv, Q. Liu, The influence of a secondary twin on the detwinning deformation of a primary twin in Mg–3Al–1Zn alloy, Mater. Sci. Eng. A 606 (2014) 81–91.
[32] J. Xu, B. Guan, H. Yu, X. Cao, Y. Xin, Q. Liu, Effect of twin boundary–dislocation–solute interaction on detwinning in a Mg–3Al–1Zn alloy, J. Mater. Sci. Technol. 32 (2016) 1239–1244.
[33] Z.N. Yang, Y.Y. Xiao, F.C. Zhang, Z.G. Yan, Effect of cold rolling on microstructure and mechanical properties of pure Zr, Mater. Sci. Eng. A 556 (2012) 728–733.
[34] H. Somekawa, H. Watanabe, D.A. Basha, A. Singh, T. Inoue, Effect of twin boundary segregation on damping properties in magnesium alloy, Scr. Mater. 129 (2017) 35–38.
[35] Y. Xin, L. Lv, H. Chen, C. He, H. Yu, Q. Liu, Effect of dislocation-twin boundary interaction on deformation by twin boundary migration, Mater. Sci. Eng. A 662 (2016) 95–99.
[36] A. Chapuis, Y. Xin, X. Zhou, Q. Liu, {10-12} Twin variants selection mechanisms during twinning, re-twinning and detwinning, Mater. Sci. Eng. A 612 (2014) 431–439.